OATAO

Open Archive Toulouse Archive Ouverte

Modeling the Hydromechanical Solution for Maintaining Fish Migration Continuity at Coastal Structures

Léo Guiot[1]; Ludovic Cassan[2]; and Gilles Belaud[3]

Abstract: To promote water control in coastal areas developed for agriculture, tidal hydraulic structures (doors and flap gates) are used for the hydraulic management of irrigation and drainage networks. By closing when the water level increases due to the tide, they prevent sea water inflow. However, fish using the tidal wave to move forward (e.g., glass eels) are also blocked from accessing the hydrologic network. There are hydromechanical solutions to mitigate these problems, such as adding a wooden block to leave an opening at high tide or adding a spring to delay the closing of the structure. The latter solution allows the structure to remain open only during a part of high tide. Designed empirically, these solutions can either alter the hydraulic control performance or be insufficiently effective for fish passage. This study proposes an operating model approach for hydromechanical structures that takes these passage solutions into account. This approach makes it possible to evaluate the performance of the passage solutions for fish passage and hydraulic regulation. With the help of these models, it is possible to design solutions that ensure a compromise between the passability of fish species and agricultural uses.

Introduction

Today's hydrographic networks are strongly anthropized, and in rivers both the water heights and the flows (Nilsson et al. 2005) are regulated. The objective of this regulation is to benefit different activities: agriculture, habitat, navigation, drinking water supply, and energy production. Hydraulic references [Chow (1959), Henderson (1966), French (1985), Sinniger and Hager (1988), among others] correctly deal with the problem of modeling standard hydraulic control structures, but structures specific to the coastal environment are rarely addressed. The presence of these structures also raises problems of ecological and fish continuity. Indeed, they constitute obstacles to the free movement of fish, which induce risks for the survival and sustainability of some fish species (amphialine fish, for example). Some structures impose local flow conditions that are impossible for fish to pass (Ovidio and Philippart 2002; Amaral et al. 2016) due to excess velocity or head barriers. To restore fish passage, fishway structures have been developed, such as fish ladders (Larinier 2002), fish lifts (Travade and Larinier 2002), and naturelike fish passes (Katopodis et al. 2001; Cassan et al. 2014). Developed in continental rivers, these solutions have proved to be very effective but are no longer relevant when the direction of the flow can change with tidal cycles as it does on the coast. Yet coastal hydrographic networks are no exception to the current strong anthropization of rivers, which is also accompanied by ecosystem degradation (Lotze et al. 2006). They also face specific management problems due to seawater intrusion. Indeed, this water is salty, which is harmful for agricultural use, and can have a high content of suspended matter, leading to sedimentation in the networks. To limit seawater intrusions, specific works have been developed (Giannico and Souder 2005), such as flap gates (top-hinged gates) and tidal doors (side-hinged gates).

However, these structures are also obstacles to fish migration (Giannico and Souder 2004). Indeed, when the current moves from saltwater areas to rivers, they close and prevent any passage for fish that wish to pass at this time of the tide (Doehring et al. 2011), such as amphialine fish, which have a physiological need to change their living environment (salt/freshwater) during their growth cycle. One such case is the elver, which have low swimming ability and use the tide-induced current to be pushed from the estuary or the sea into the waterways (McCleave and Kleckner 1982), as do many species (Gibson 2003).

This is the case for *Anguilla anguilla*, an economically and ecologically important species. Its population has decreased dramatically since 1980, leading the International Union for Conservation of Nature (IUCN) to declare it as an endangered species. Obstacles to migration due to hydraulic structures is one of the major reasons cited for this decline (Feunteun 2002). Indeed, glass eels, one of the juvenile stages of *Anguilla anguilla*, have a burst swimming speed of 0.6 m/s (McCleave 1980) and use the tide to move from the estuary to the upstream river systems (McCleave and Kleckner 1982). Solutions to improve passability are based on keeping an opening during all or part of the tide. These solutions are used in France in some freshwater marshes along the Atlantic coast in order to improve the passage of glass eels at tidal gates (Rigaud 2015). Field measurements demonstrated that elvers were able to move from the estuary to freshwater marsh at tidal gates with small

[1]Institut de Mécanique des Fluides de Toulouse, allée du Prof. Camille Soula, Toulouse 31400, France; Pôle R&D écohydraulique, Office Français de la Biodiversité-Institut de Mécanique des Fluides de Toulouse-Recherche pour l'ingénierie en matériaux, mécanique et énergétique pour les transports, l'énergie et l'environnement, allée du Prof. Camille Soula, Toulouse 31400, France (corresponding author). Email: guiotdeleo@gmail.com

[2]Assistant Professor, Institut de Mécanique des Fluides de Toulouse, allée du Prof. Camille Soula, Toulouse 31400, France; Pôle R&D écohydraulique, Office Français de la Biodiversité-Institut de Mécanique des Fluides de Toulouse-Recherche pour l'ingénierie en matériaux, mécanique et énergétique pour les transports, l'énergie et l'environnement, allée du Prof. Camille Soula, Toulouse 31400, France.

[3]Professor, UMR G-eau, Univ. of Montpellier, AgroParisTech, Cirad, Institut Agro, Institut national de recherche pour l'agriculture, l'alimentation et l'environnement, Institut de Recherche pour le Développement, 2 place Pierre Viala, Montpellier 34060, Cedex 1, France.

openings, whereas they were blocked by gates completely closed (Rigaud et al. 2014).

These adaptations have a hydraulic influence even upstream of the network, due to backwater effect. It is therefore necessary to make a compromise between ecological continuity (fish migration) and the hydraulic functionality of the network (water level and water quality). To find this compromise, it is therefore essential to be able to dimension the hydromechanical solutions and their impact.

The objective of this study is to develop an original modeling approach for hydromechanical structures under the influence of the tide in order to evaluate and compare adaptations of these structures for fish passage.

After a review of the water management structures present in tidal rivers, models of hydromechanical structures including passage solutions are introduced. Their application is presented on a typical case of coastal areas. The results are then discussed with a view to their application to other contexts.

Tidal Gates and Fish Migration

Functioning Principles

The regulation of flows between the marine environment and the coastal hydrographic network meets several different needs. It may be a way of limiting only the inlets to avoid flooding or to preserve an estuarine ecosystem. For agriculture, the aim is usually to stop salt intrusions from the sea and maintain high water levels for irrigation. Tidal conditions, with fluctuating downstream water level and water quality, impose specific constraints on regulating structures which involve variations in opening according to the tide.

Structures connected to the sea (Fig. 1), used to prevent these issues, are generally flap gates (top-hinged) or tidal doors (side-hinged). In normal operation, hydromechanical structures close when water levels are reversed. Tide gates can be associated with other structures to regulate the flow when open. For this reason, a sluice gate or weir is usually found a few meters upstream of a tide gate. A review of this type of structure is available in Rampano (2009).

Available Solutions for Passability

Tidal gates also have an impact on fish passage. For certain species of fish this amounts to a complete blockage, because they only move at high tide.

The simplest solution to restore the free movement of fish is to keep an opening in the structure that allows fish to pass through it. This can be done with the help of a fixed opening or a block that prevents the structure from closing completely. The disadvantage of these solutions is the admission of volumes of salt water and suspended matter that could hamper the functionality of the network. In addition, the admission of salt water creates a rise in the water level upstream of the structure, which can also hinder the drainage function. To limit the volume of salt water admitted to the network at high tide, hydromechanical solutions can open or close the orifices, depending on the water levels. With a spring (Lauronce et al. 2015) or float system with counterweight, it is possible to delay the closing and allow time for fish passage.

Closure retarders do not keep the tide gate open to the sea during high tide. There is always a temporary interruption in ecological continuity, but it is not as long. Trancart et al. (2012) has shown that, in some estuaries, fish species with low swimming ability take advantage of the first few hours of tidal inversion to make use of the current induced by the flow. This is also the case for other species Becker et al. (2016), for which closure retarders will also have a positive impact.

Other, more complex systems of self-regulating gates exist (self-regulating tide gates, or SRT gates). Waterman float-type gates or regulator of tidal exchange (RTE) gates (Taylor 2011) can also be described by a law giving the opening as a function of the downstream water level.

It can be mentioned that for endangered species such as manatees, gate management using an acoustic detection sensor system has also been developed to avoid their mortality (O'Shea et al. 1985).

For the sake of simplification, we will focus on three types of gates for the study of passage adaptations: tidal doors (TD), flap gates (FG), and SRT. The method proposed can be easily adapted to other gates if the relationship between the opening and the water level is known.

Fig. 1. (Color) Example of tidal door at Charras marsh.

Materials and Method

Experimental Device

To demonstrate the performance of the passage devices (springs and floats, applied on different types of gates), the approach is illustrated on the Charras marsh, a medium-sized marsh on the French Atlantic coast. The structure provides control between the Charente estuary and a 5-m-wide channel at the bottom (width of the gate), with a riverbank slope of (m) 4, 7.5 km long, with tidal ranges from 2 to 4 m and upstream inflows (Q_m) of up to 10 m³/s. Upstream of the modeled channel, the flow is assumed to be constant per period, because the inflow results from drainage of the watershed. The hydraulic control structure consists of two separate, parallel reaches, each equipped with a tidal door and a 2-m-wide sluice gate. Only one of the two gates is equipped with a block, keeping a minimum opening of 20 cm. Level probes were installed (1) downstream of the door, (2) between the door and the gate, and (3) upstream of the control gate (Fig. 2). They record the water level in 10-min time steps. The measurement periods extend over several months in 2015 and 2018. Several consecutive tides with different tidal ranges will be considered. Flow measurements were carried out with an acoustic doppler current profiler (ADCP, Teledyne RD Instruments, Daytona Beach, Florida) during several tides, upstream of the control structure, with a sampling time of 15–30 min.

Water Level Regulation and Opening Calculation

Marshland management generally involves maintaining a consistent water level. For this purpose, the hydromechanical tide gate is coupled to a sluice gate, which can be limiting for the flowrate at low tide. We will therefore consider the complete hydromechanical structure including the gate. The upstream condition will be the daily flow of the marsh Q_m. An iterative calculation allows us to obtain, for each value of Q_m, the opening of the W gate, which ensures the mass conservation on the section. This makes it possible to compare the different devices under the same hydrological conditions. Note that the gate is the structure that limits the flow when it occurs from the marsh to the sea. Unlike regulation gates, the structure to limit salt intrusion offers little head loss, which can be neglected. As a consequence, knowledge of their opening is not required when water flows toward the sea.

To estimate the flow passing through the combined structure (structure + gate), noted as Q_{sea}, we will calculate the flow passing through the hydromechanical structure to the sea and the flow passing through the gate. Each of these flows is calculated by considering as unknown the water height h_i in the lock chamber. An iterative calculation is used to find the value of h_c which equals the flows in the tide gate and under the sluice gate at each time step.
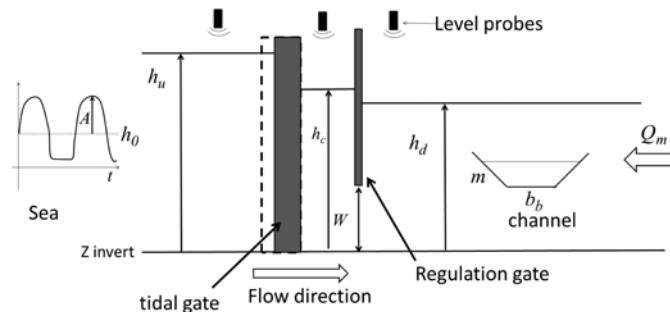

Fig. 2. Diagram of installation with a control gate (example of a tidal door) for a flow from the sea to the channel.

This is equivalent to considering a rapid filling of the chamber in order to neglect the unsteady effects. This assumption is justified by the small volume of the chamber in relation to the inflow and outflow.

Numerical Method

Computation of the flow rate at the sluice gate must take into account transitions due to current reversals when the gate is submerged. We have therefore adopted the approach developed by Belaud et al. (2009) to ensure continuity between the different regimes, which is not the case with conventional formulations considering a constant contraction coefficient.

For the hydromechanical structures (flap gates or doors), the laws developed by Burrows et al. (1997) make it possible to represent the flowrates from the marsh to the sea. However, the addition of passage devices induces reverse flows (from the sea to the marsh). Specific laws must then be developed.

The tide has an impact on the hydrographic network upstream of the tide gate, and to represent the tidal range induced, a trapezoidal-shaped open channel is used. It can model either a real reach or a more complex storage volume (network). Temporal variations in its volume V must satisfy the continuity equation

$$\frac{\partial V(t)}{\partial t} = Q_m - Q_{sea}(t) \tag{1}$$

$$L \frac{dh_d(t)}{dt}(b_b + 2mh_d(t)) = Q_m - Q_{sea}(t) \tag{2}$$

where V = volume of water in the channel; h_d = height of water in the channel; L = length of the channel; m = slope of the riverbanks; b_b = width at the bottom; and Q_{sea} = flowrate from the sea. The flowrate upstream of the marsh, Q_m, is imposed as a boundary condition. The downstream condition is provided by a 12-h period synthetic tide. It is defined by its amplitude A and mean value h_0 (Fig. 2). Because the structures are installed in an estuary, the low tide is truncated at a constant value corresponding to the flow from the regulation gate. This water level is assumed to be constant because the structure is open and the gate operates in a free flow condition. This assumption therefore has no influence on the flow calculation.

Finally, the model proposed is well represented by Fig. 2, where the tidal gate is modeled with considerations presented in the following section. The resolution of the structure equations and Eq. (2) is done by a finite difference diagram (of order 1) with a time step of 20 s.

Modeling of Tide Gate Modifications for Fish Passage

In this article, we illustrate the modeling of assisted passage devices considering square flap gates and rectangular doors. The same methodology will be applied to more complex structures (circular) simply by modifying the expression of forces according to the geometry studied.

Tidal Door and Stiffener

The purpose of a stiffener is to limit the closing of the structure when the door is subjected to greater pressure on the seaward side (Laurence et al. 2015). When the current reverses, the door starts to close. It is stopped by the presence of a stiffener, which will then compress as the difference in level between the sea and the marsh increases. When the sea-side water level drops, the pressure on the
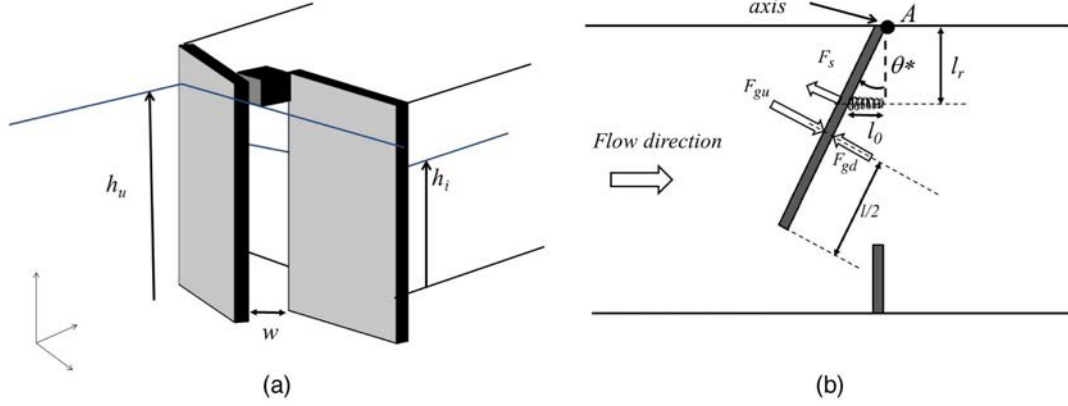
Fig. 3. Diagram of a tidal door with (a) a block or (b) a stiffener.

gate decreases, so it starts to open. If it rises sufficiently, the pressure on the gate may be sufficient to compress the spring until the gate is completely closed.

To know the opening for a given submergence, one writes the balance of the moments on the gate. The stiffener is installed along the x-axis at a distance l_r from the bank. The no-load length is denoted l_0 and its stiffness k. The door is only in contact with the stiffener when it closes for $\theta^* = a\tan(l_0/l_r)$ (Fig. 3). θ is defined in the clockwise direction.

The theorem of angular momentum allows the stiffener force (f_x) to be linked to the hydrostatic forces on the door (Appendix). F_{gu} is the pressure force exerted by the water on the upstream plane, F_{gd} is the pressure force exerted by the water on the donwstream plane, and F_a is the pressure force exerted by the air on the donwstream plane. It is assumed that the link between the stiffener and the door is a point without friction (see Appendix)

$$F_{gu}\frac{l}{2} + F_{gd}\frac{l}{2} + F_a\frac{l}{2} + \frac{f_x}{\cos\theta}\frac{l_r}{\cos\theta} = -\frac{d}{dt}(J_A\dot\theta) \quad (3)$$

$$\left(p_0 h_u + \frac{1}{2}\rho g h_u^2\right)l\frac{l}{2} - \left(p_0 h_d + \frac{1}{2}\rho g h_d^2\right)l\frac{l}{2} - (p_0 h_u + p_a h_d)\frac{l}{2}$$
$$+ kl_r^2(\tan\theta - \tan\theta^*)(1 + \tan^2\theta) = -\frac{d}{dt}(J_A\dot\theta) \quad (4)$$

where p_0 = atmospheric pressure; and J_A = moment of inertia with respect to the vertical axis passing through A. Considering the door as a rectangular parallelepiped of thickness e, we obtain $J_A = 4m/3(e^2 + l^2)$ with m being the mass of the door

$$\frac{1}{2}\rho g(h_u^2 - h_d^2)\frac{l^2}{2} + kl_r^2(\tan\theta - \tan\theta^*)(1 + \tan^2\theta) = -J_A\ddot\theta \quad (5)$$

$$\frac{1}{4}\rho g h_u^2(1 - X^2) + k\left(\frac{l_r}{l}\right)^2(\tan\theta - \tan\theta^*)(1 + \tan^2\theta) = -\frac{J_A\ddot\theta}{l^2}$$
$$\qquad (6)$$

$$\frac{(1 - X^2)}{4} + \tilde{k}\tilde{l}^2(\tan\theta - \tan\theta^*)(1 + \tan^2\theta) = -\frac{J_A\ddot\theta}{\rho g h_u^2 l^2} \quad (7)$$

where $\tilde{k} = k/\rho g l^2$ is the stiffener constant that depends only on the geometric configuration of the device and $\tilde{l} = (l_r/h_u)$ depends on the sea water level.

We will verify in the following that the quasi-stationary solution ($J_A = 0$) is sufficient to describe the incoming volume. Although the following results are presented for the complete quasi-stationary

resolution, it can be noted that the solution for small θ angles allows us to obtain an analytical expression of θ giving almost identical results:

$$\tan(\theta) = -\frac{(1 - X^2)}{4\tilde{k}}\tilde{l}^2 + \tan(\theta_*) \quad (8)$$

The device with stiffener therefore allows to keep an opening w which can be expressed as a function of the opening angle θ

$$w = l\sqrt{2(1 - \cos(\theta))} \quad (9)$$

Thus the flow rate is obtained by considering a vertical slot law [Eq. (10)]

$$Q = C_d w h_u \sqrt{2g(h_u - h_d)} \quad (10)$$

The value of C_d can be deduced from the energy balance realized on a volume of water delimited by an upstream section and the contracted section in the slot. It is assumed that the head loss between the inlet and the outlet is negligible; the dissipation mainly occurs in the jet downstream of the slot. This equation should allow us to know the flow coefficient, C_d, as a function of the hydraulic conditions and the velocity distribution at the limits of the control volume. The energy balance is therefore written as

$$h_u + \alpha_u\frac{1}{2g}\left(\frac{Q}{Bh_u}\right)^2 = h_d + \alpha_d\frac{1}{2g}\left(\frac{Q}{wC_ch_d}\right)^2 \quad (11)$$

where C_c = ratio between the flow passage width and the door opening; and α_d and α_u = Coriolis coefficients due to the transverse heterogeneity of the velocities over the width B (upstream) and Ccw (downstream), respectively. For the continuation, one supposes $\alpha_u = 1$. Using numerical simulation, Cassan et al. (2018) showed that we could consider $C_c = 0.75$ and $\alpha_d = 1.05$.

Eq. (11) can be put into dimensionless form by defining $F_0 = Q^2/gB^2h_u^3$, $X = h_d/h_u$, and $a = w/B$

$$1 - X = \frac{1}{2}F_0^2\left(\frac{\alpha_d}{(aC_cX)^2} - 1\right) \quad (12)$$

Thus the flow coefficient is written as

$$C_d = \frac{F_0}{a}\frac{1}{\sqrt{2(1 - X)}} \quad (13)$$

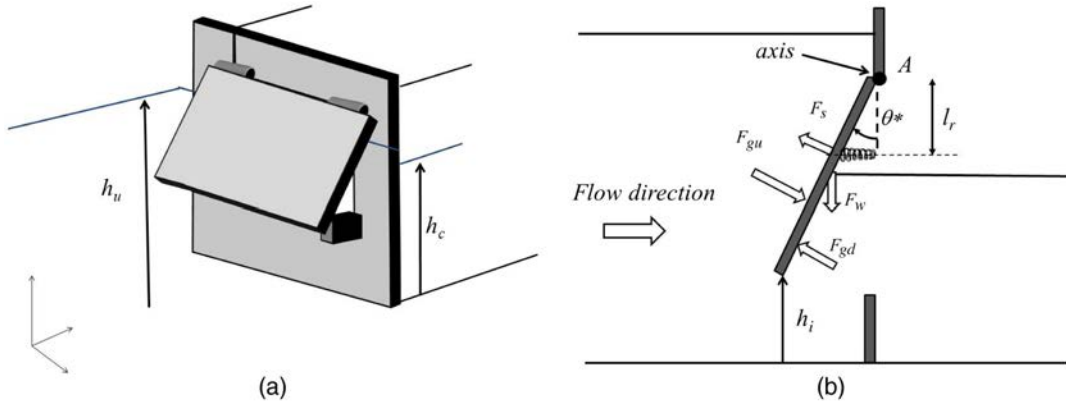The flow through the slot can then be obtained by coupling Eqs. (10) and (13).

Fig. 4. Diagram of a flap gate with (a) a block or (b) a stiffener.

Flap Gate and Stiffener

The main difference with the tidal gate is that the axis of rotation is horizontal (Fig. 4). In addition, when the flow is toward the sea, the flap exerts a resistance to the flow. We consider that in this case, the flow is limited by the upstream management gate and the water level between the two structures is equal to the downstream level.

The dimensioning of a stiffener for a flap gate is also based on the angular momentum theorem, as previously noted. Strictly speaking, the pressure on the upstream face of the gate is not hydrostatic near the separation point. However, the calculation of the flow from the sea to the upstream side is done when the gate submergence is large ($h_u \approx h_d \gg w$), which limits the deviation to the hydrostatic pressure.

The angular momentum is written as

$$M_u + M_d + M_w + M_s = -J_A \ddot{\theta} \tag{14}$$

where M_w = moment of the weight and is expressed by assuming a rectangular parallelepiped, i.e., a center of gravity at $l/2$; and M_u, M_d, and M_s are the moment due to the force on the upstream plane of the gate, on the downstream plane of the gate, and due to the stiffener respectively.

We denote $X_s = h_{su}/hu$, $X_i = h_{sd}/hu$, $X_d = h_d/hu$, and $X_A = h_A/hu$. Then Eq. (14) becomes (see Appendix)

$$(X_{su} - X_i)\left\{ X_A - \frac{1}{2}(1 + X_A)(X_{su} + X_i) + \frac{1}{3}(X_{su}^2 + X_i^2 + X_{su}X_i) \right\}$$

$$- (X_{sd} - X_i)\left\{ X_d X_A - \frac{1}{2}(X_d + X_A)(X_{sd} + X_i) \right.$$

$$\left. + \frac{1}{3}(X_{sd}^2 + X_i^2 + X_{sd}X_i) \right\} + \frac{1}{2}\tilde{m}\sin\theta \tilde{l}^3$$

$$+ \tilde{k}\tilde{l}^3(\tan\theta - \tan\theta^*)(1 + \tan^2\theta) = -\frac{J_A\ddot{\theta}}{\rho g h_u^3 l} \tag{15}$$

where $\tilde{m} = m/\rho h_u^2 l$ and $\tilde{l}$ and $\tilde{k}$ have the same definition as for the tidal door. It can be noted that compared to the tidal door, the term $\tilde{l}$ is to the power of 3 because the moments are here integrated on the vertical. The upstream h_{su} and downstream h_{sd} integration bounds depend on the relative position of the heights with respect to the rotation axis.

If the water level is higher than the rotation axis $h_{su} > h_A$, then $h_{su} = h_A$; otherwise, $h_{su} = h$. Thus there are three possible cases:
- $h_d < h_u < h_A$: all heights are less than h_A
- $h_d < h_u$: heights are on either side of h_A
- $h_A < h_d < h_u$: all heights are greater than h_A

In a quasi-stationary state, Eq. (15) becomes

$$A_1 - A_2 + \frac{1}{2}\tilde{m}\sin\theta \tilde{l} + \tilde{k}\left(\frac{l}{h_u}\right)^2(\tan\theta - \tan\theta^*)(1 + \tan^2\theta) = 0 \tag{16}$$

where A_1 and A_2 = terms of the first and second line of Eq. (13).

The flowrate at the flap gate in the upstream direction is assumed to be similar to the flowrate under a sluice gate, whose opening w is given by Eq. (17). The discharge coefficient C_d of this structure may differ from those in conventional use because here the inclination of the flap gate is toward the upstream side of the flow. For this reason, we choose to use a vertical sluice gate law to compute the discharge (Belaud et al. 2009)

$$w = b\sin\theta = l\sqrt{2(1 - \cos\theta)}\sin\theta \tag{17}$$

It is possible to obtain two borderline cases with the structure + stiffener models:
- Structure with block: To obtain it, we simply solve the equations with an infinite stiffener constant $\tilde{k}$. The size of the block is therefore the size of the spring l_0. This solution can be used for tidal doors as well as for flap gates.
- Structure without modification: This is the case where the structure is not equipped with a hydromechanical passage device. To obtain it, we solve the equations with a zero spring size ($l_0 = 0$). This solution can be used for tidal doors as well as for flap gates.

Flap Gate and Float

There are a large number of devices for improving the ecological continuity of tide gates. They often involve floats that control the closure of the gate at the upstream or downstream level (Bernhard and Perona 2017; Belaud and Litrico 2008). To illustrate the approach, we select one of these devices, published under the name "mitigator fish-passage device" [invented by Giannico and Souder (2005)], which is equivalent to stiffeners in terms of simplicity, construction cost, and adaptability to a wide variety of situations.

The mitigator fish-passage device is a closing delay device with a cam. When the current reverses, the flap starts to close but a cam linked to a float holds the door closed completely. If the float is raised (and the downstream water level is below the float), the cam does not move and prevents the flap from closing completely like a fixed block. When the water level reaches the float, the hydromechanical device actuates the cam so as to progressively decrease
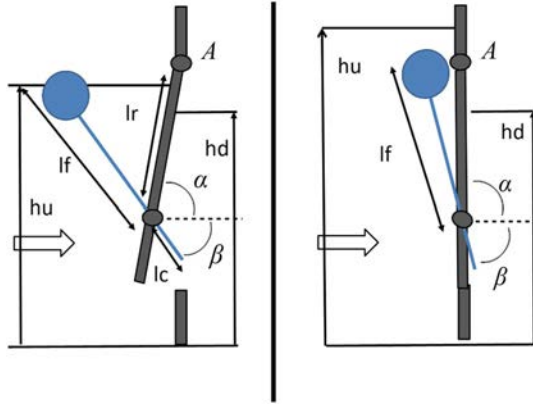
Fig. 5. This picture represents two schema of an SRT device when $h_u > h_d$, first before the float is submerged and then when the float is submerged.

the opening of the flap as the water level rises. When the float is completely submerged, the cam no longer keeps the gate open and therefore it is completely closed (Fig. 5). In this device, once the current has been reversed, the opening of the flap is only controlled by the sea water level, unlike the device with a stiffener. This system is therefore independent of the management level in the network (h_d).

The dimensioning of the float device for a gate is based solely on geometrical considerations. The opening angle of the flap is based on the water level in the estuary (i.e., downstream of the structure). When the current has reversed there are three possible cases:

- Estuary level < minimum float level: $\theta = \theta_*$ (θ_* is the angle left by the hold that leaves an opening as long as the float is not submerged)
- maximum float level > estuary level > minimum float level: $\theta = f(h_u)$ [$f(h_u)$ is deducted from the equation in this part]
- Estuary level > maximum float level: $\theta = 0$

In practice, the device is dimensioned such that the second case lasts only a short time, so that it behaves either open or close. Nevertheless, we develop here the complete calculation which allows to show the method for any type of SRT—for example, for the more complicated function $f(h_u)$.

The trigonometrical and geometrical relations described in the Appendix bring the following equation:

$$h_A - h = l_r \cos\theta - l_f \sqrt{1 - \left(\frac{l_r}{l_c}\sin\theta\right)^2} \tag{18}$$

In order to know when the float has emerged, it is necessary to determine the height the float is at when $\theta = \theta^*$. This allows us to calculate the corresponding β^* angle

$$\beta^* = \arccos\left(\frac{l_r}{l_c}\sin\theta^*\right) \tag{19}$$

So we get the possible minimal water level ($h_{float,\min}$):

$$h_{float,\min} = h_A - l_r \cos\theta^* - l_f \sin\beta^* \tag{20}$$

Finally, the maximum level to which the float can rise is determined. This gives us the immersion limit. The maximum level of the float is when $\theta = 0$ and $\beta = 90°$. So we have

$$h_{float,\max} = h_A - l_r + l_f \tag{21}$$

As with the flap gate and stiffener solution, the flow is similar to that through a sluice gate, whose w opening is given by Eq. (17).

Quasi-Stationary Hypothesis

To ensure the validity of the quasi-stationary solution with a stiffener, we take the case of the Charras tide gate with $l_r = l = 2$ m, $m = 1{,}000$ kg, and $e = 0.2$ m (Fig. 6). The complete equations [Eqs. (7), (10), and (13)] are thus solved numerically as a function of time for the floating gate using a Runge Kutta scheme of order 4. On the other hand, the quasi-stationary solution (Q_S) where J_A is assumed to be zero is also obtained [Eq. (16)]. We notice that the complete solution causes oscillations in the system but the flow rates and apertures are similar between the two types of resolutions. In practice, the oscillations could be suppressed by adding a viscous term to the stiffener (damper type). For the knowledge of flow rates, we assume that quasi-stationary resolutions are sufficient.

From the reversal of the current, the flow increases with the sea level until the opening is zero. The stiffness $\tilde{k}$ is used to change the time of complete closure. When the stiffness is low, the door closes quickly, allowing little water to enter. On the other hand, for high stiffnesses, the opening angle remains almost constant. In this case,
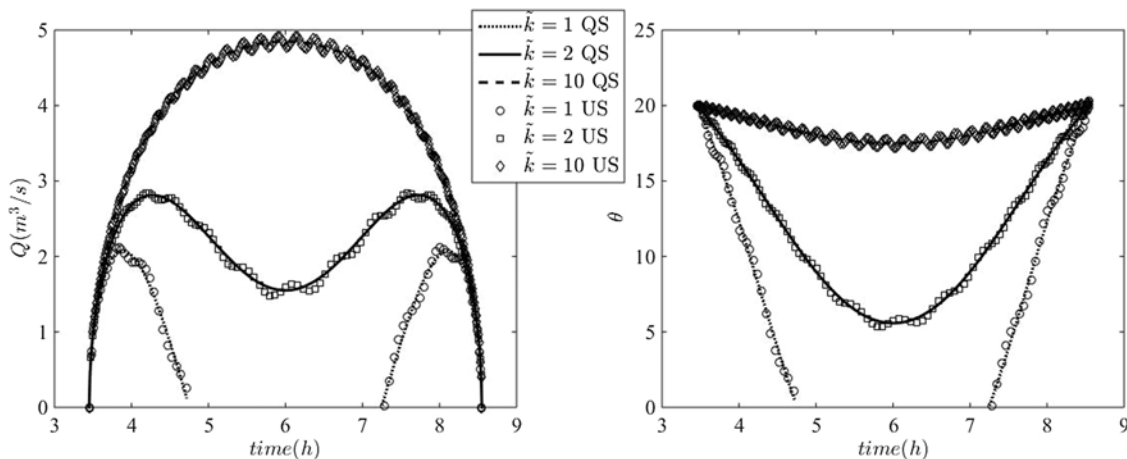

Fig. 6. Comparison of complete and quasi-stationary solutions for a door in the water.

the hydraulic behavior of a floating door with a fixed block is the same as in the case of Charras. The use of the stiffener thus makes it possible to give priority to passage times at the beginning and end of the inversion while limiting the total volume admitted into the marsh.

Calibration

To evaluate the method in the case of a block device, we select several consecutive tides in 2015 and 2018 with different tidal co-efficients. The downstream condition (sea) is the measured condition and the upstream flow rate is the mean daily flows obtained from measurements as described previously. Using upstream and downstream probes and openings, these measured flowrates are calculated by applying the flow laws defined previously. With regard to the flowrate (Fig. 7), the structures are calibrated on the more time-defined 2015 data. To obtain these results, the law of Belaud et al. (2009) is used with a zero head loss coefficient, and the discharge coefficient of the tidal door is 0.8. For 2018, although the discharges are of the right order of magnitude, we obtain deviations of the order of 10% from the measurements. As the measurement was made just after a change in gate opening, it is likely that transient effects are disturbing the measurement. Fig. 7 clearly shows the increase in flow rate over the period and the management which is operated manually approximately every 2 days.

Sensitivity Study

To highlight the model sensitivity as a function of the parameters, we consider the experimental case with a daily flow of 3 m³/s. The comparison of the hydrographs (Fig. 8) for several blocks allows us to show that they have an influence on the hydraulics.

Indeed, in order to discharge a constant daily flow, the maximum flow rates can vary by more than 30% even for small block sizes (20 cm). In the same way, the block induces significant extra level in the network if no other management action is implemented. It can be noted that taking into account variation of network level implies a different time for flow reversal. It also causes an asymmetry in the flows when the flow goes toward the sea. The ratio of inflow (V_{in}) and outflow (V_{out}) is visualizable on the hydrographs because they correspond to the area under the curve when the flow is negative and when it is positive, respectively. As expected, a larger block increases this ratio, because the method is made so that the volume from upstream is always discharged regardless of the volume entering from the sea.

The measurements also make it possible to interpret the influence of block size. Although the increase in block size results in a few centimetres of extra level, this is still small compared to the total tidal range observed in the network. In the case of Charras with a 20-cm block, the V_{in}/V_{out} ratio is between 0 and 0.2 (the variation depends on the tidal range, upstream flow, and management), with no observed significant impact on the ecology nor on the current water uses. Agreement between the measurement and simulation is better in 2018 (Fig. 9). This difference can be explained by dredging work that modified the cross sections before the measurements. The differences are more likely to be observed at low water level, because measurements are generally 10 cm lower than the averaged level of the network due to the hydraulic gradient caused by high flows. This difference from the assumption of parallel bottom level could explain the discrepancies between models and measures.

It can also be seen that the tidal range is not linear in the measurements, unlike in the simulations. This difference can be
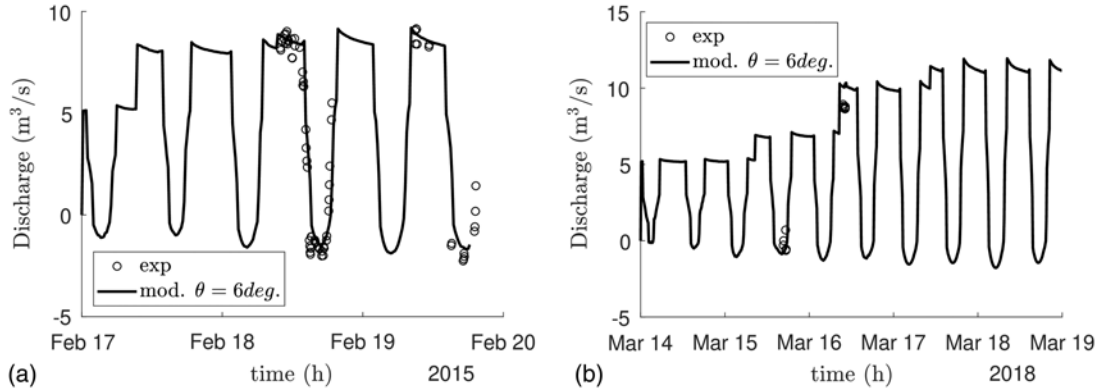

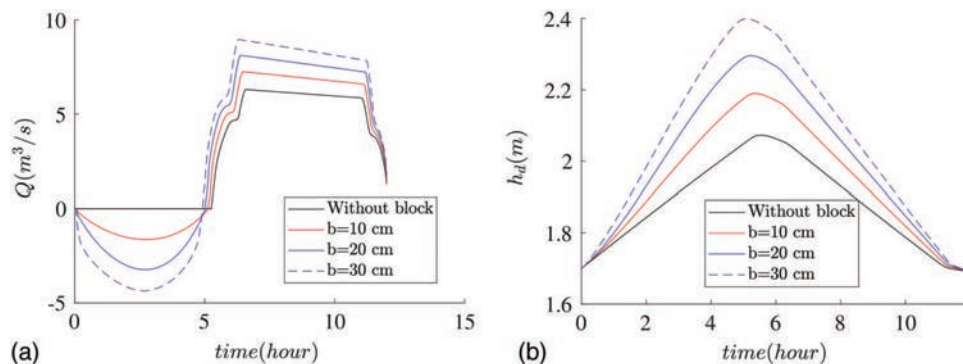Fig. 7. Comparison of measured and simulated flows upstream of the Charras structure.

Fig. 8. (Color) Comparison of hydrographs and simulated water levels upstream of the Charras structure as a function of the size of the hold.
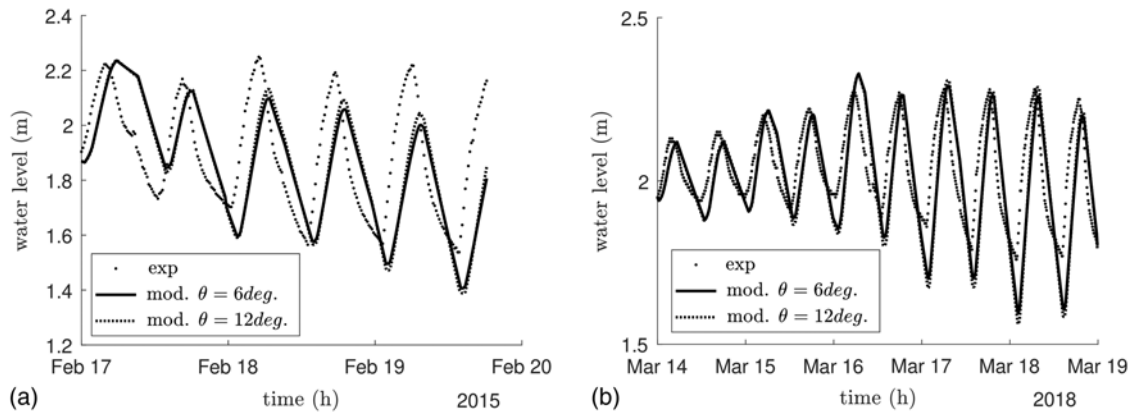
Fig. 9. Comparison of measured and simulated dimensions upstream of the Charras work.
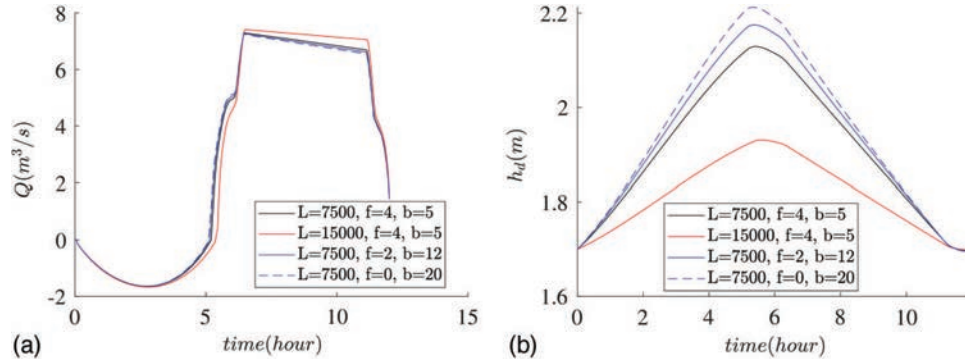

Fig. 10. (Color) Comparison of hydrographs and simulated water heights upstream of the Charras structure according to the size of the hold.

explained by the nontrapezoidal geometry of the canal or a non-constant Q_m flow (another storage channel is present upstream). However, it is also possible that lateral inflows distributed along the channel play a role because their dynamics are different.

Finally, the good agreement of the measurements with the experiment shows a good simulation of the storage effect in the network. The channel length (7,500 m), bottom width (5 m), and slope bank (4) were obtained from bathymetric surveys in 2018. However, because an averaged value is required for the model, it was obtained by fitting it to the experimental measurements in 2018. Measurements are not always available, though, so we look at the influence of geometry on the simulations.

According to Fig. 10, to reduce the level variation in the network significantly, the length of the reach must be multiplied by at least 2 ($L = 15,000$ m instead of 7,500 m). Even though the hydrographs are rather identical for all cases, it can be seen that taking the reach into account provides important management information, i.e., the possible overtopping due to passage solutions. For a same mirror width (20 m), the shape of the channel (b and f) also has an influence of about 15 cm on the water level. This value is close to the maximum uncertainty allowed for conventional management. Consequently, it seems important to consider the most realistic geometry possible if a calibration cannot be made.

Results

Impact of Variability in Hydrological Conditions

The increase in the upstream Q_m flow rate leads, for all solutions, to a decrease in the inflow/outflow volume ratio for each device

(Fig. 11). This evolution is explained by the choice to maintain a fixed average level on the network. The regulating gate would be more or less open to allow the upstream flow to pass through. On the other hand, the incoming volume is still determined by the water level and the structure at sea. The fact that V_{in} remains almost constant when V_{out} increases explains the lower ratio. However, the advantage of the proposed modeling is that the increase in levels and volumes can be quantitatively calculated.

Fig. 12 shows the impact of tidal range variation on the inflow/outflow volume ratio of each device. Tide gates with stiffeners and gates with SRT devices exhibit a maximum of inflow/outflow
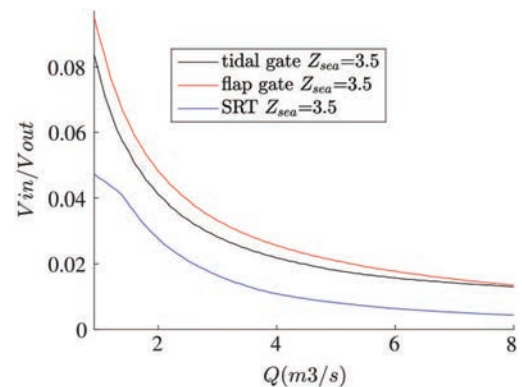

Fig. 11. (Color) Influence of upstream flow Q_m on the volume ratio and H_{bief}. The stiffeners have the same $\tilde{k} = 3$, $\theta = 10$. For SRT, $l_r = 0.5$ m, $l_c = 0.3$ m, and $l_f = 0.2$.
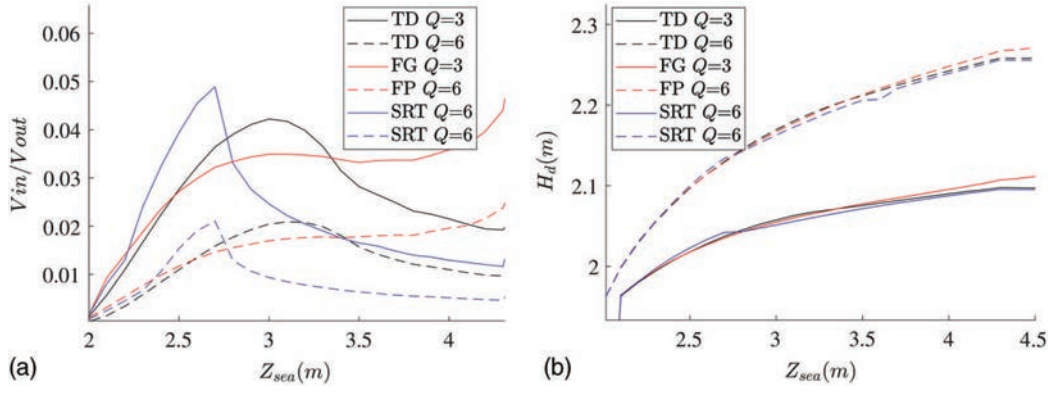
Fig. 12. (Color) Influence of the tidal range $\Delta H/r$ and the average of h_d for three different flowrates. The stiffeners have the same dimensionless stiffness of 3, $\theta = 10$. For SRT, $l_r = 0.5$ m, $l_c = 0.3$ m, and $l_f = 0.2$.
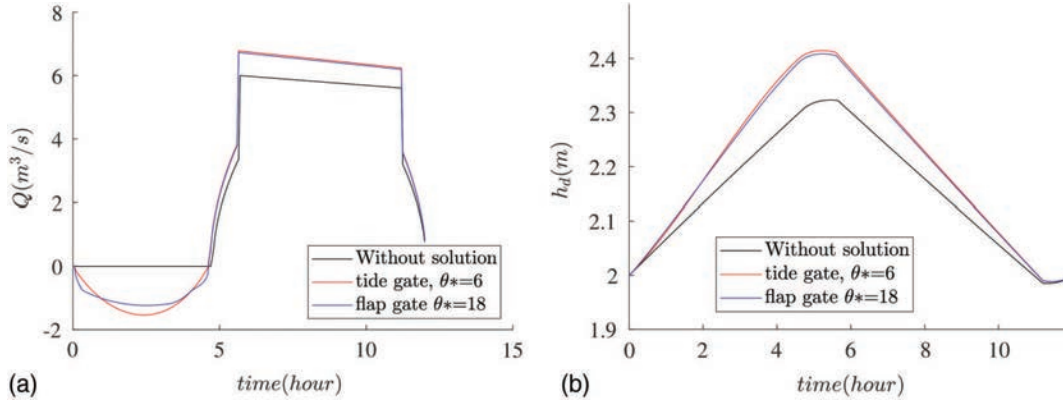

Fig. 13. (Color) Comparison of hydrographs, and of the evolution of the upstream height, for water gates equipped with a crossing system. The upstream flow is 4 m/s and the tidal range is 3.5 m. The stiffeners have the same dimensionless stiffness of 3.

volume ratio regardless of the daily upstream flow Q_m. The maximum tidal range with the higher ratio is 3 m for gates with a stiffener and 2.5 m for gates with SRT. This is the tidal range at which the devices allow the structures to be closed completely during high tide. The incoming water volume then decreases compared to the case where the structure was partially open during the whole tide. The value of this limit depends on the characteristics of the hydromechanical device (θ^*, $\tilde{k}$, and l_r). The peak of the inflow/outflow volume ratio is not visible for the flap gate with a stiffener in Fig. 12, because the stiffener has a $\tilde{k}$ too large to close the flap at the tides tested. For tidal ranges between 3 and 4 m as observed in the example, we notice that the volume ratio can increase by a factor of 2 depending on the tide in the case of a flap gate. This increase is greater (about 3) in the case of SRT. Here the devices are not optimized, but it can be noticed that the evolution of the volume ratio according to the tide can clearly be a criterion for the design and choice of the device.

Solution with Block

Fig. 13 shows the hydrographs and water level variations in the channel for solutions with fixed blocks. In order to obtain comparable solutions in terms of flow and volumes, the opening angle of the flap is three times greater than that for the tidal door. The data for the structures can be found in Table 1.

As seen previously, the block implies negative flows and therefore an increase in the maximum flow to be able to discharge this

Table 1. Characteristics of hydraulics structures

Hydraulics structure type	Width (m)	θ^* (degrees)	$\tilde{k}$	Other parameter
Tidal door	2	6	3	$l_r = l = 2$ m
Flap gate	1.5	18	0.3	$l = 1.5$ m
—	—	—	—	$h_A = 3$ m
—	—	—	—	$m = 3{,}000$ kg
SRT	1.5	18	—	$l = 1.5$ m
—	—	—	—	$l_r = 1.2$ m
—	—	—	—	$l_c = l_f = 0.5$ m

volume during the tide. The opening of the regulating gate increases from 34 cm without block to 40 cm with bock to stabilize the channel water level. The channel has high level variations due to storage. However, the presence of the passage device increases the maximum level by only 10 cm. With the flap gate, the flow that can push the elvers ($t \approx 0$ h) is greater, which is favorable to passage continuity. Nevertheless, the difference with a tidal gate remains small.

Solution with Hydromechanical System

Fig. 14 shows the hydrographs and water level variations with hydomechanical solutions (stiffener or SRT). As described before, stiffeners make it possible to reduce flows or even cancel them when k is low enough to achieve complete closure. The use of
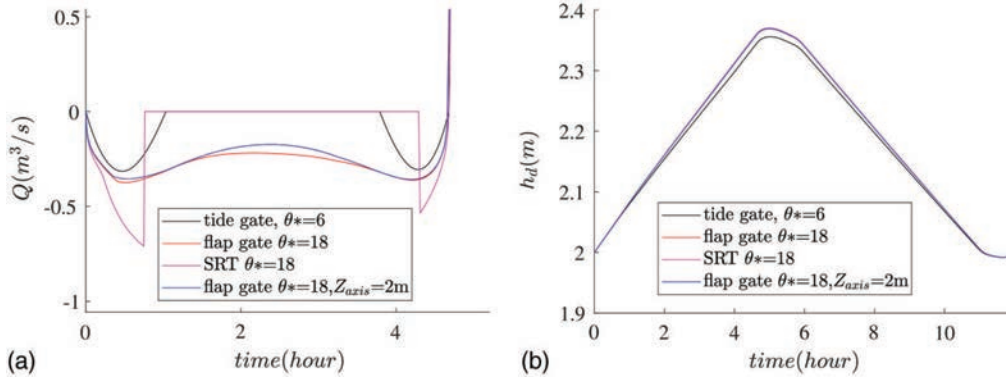
Fig. 14. (Color) Comparison of hydrographs, and of the evolution of the upstream height, for water gates equipped with a crossing system. The upstream flow is 4 m/s and the tidal range is 3.5 m. The stiffeners have the same dimensionless stiffness of 3.

stiffeners therefore makes passable periods at the beginning and end of inversion while limiting the total volume admitted into the marsh. The effect of the tidal range on the dissymmetry of the flows is identical to the case with blocks.

The SRT device works like a removable block when the water level downstream of the structure exceeds a certain level. It can be seen that, with a stiffener or SRT device, the inflows coincide with the start of negative flows. However, the flap gate remains open (k large), while it closes with the SRT device.

It can also be noted that the position of the rotation axis of the flap (h_A) changes the shape of the hydrograph for a given k stiffness. It is therefore a modifiable parameter for dimensioning.

Optimization of Devices

We have just seen that the choice of a stiffness could modify the volumes passing through. The other important parameter is the initial opening. Here we will evaluate the possibilities of optimizing these two parameters.

The size of the block, the spring for stiffener devices, or the cam for SRT devices determine the value of θ^*. Its increase induces water inlets at higher tide (Fig. 15). It is possible to choose an opening angle giving an inflow/outflow volume ratio V_{in}/V_{out} set according to environmental objectives. In Fig. 15, we can see that the reduction of the stiffness (or the reduction of the height of the float) allows the volume ratio to be reduce. For a given stiffener, the value
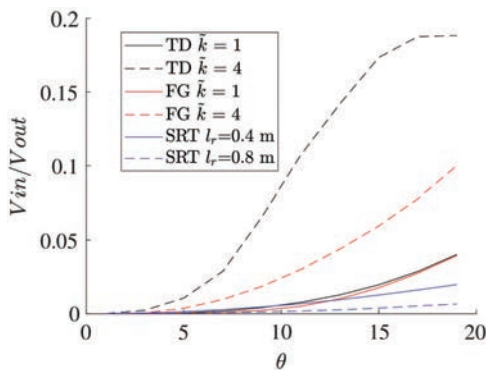

Fig. 15. (Color) Influence of angle θ on the volume ratio for two different $\tilde{k}$ stiffnesses or two different l_r lengths. The upstream flow is 3 m³/s and the tidal range is 3.5 m.

of $\tilde{k}$ (or the position of the float) can easily be changed by moving it closer or further away from the axis of rotation.

For devices based on stiffeners, the impact of the value of $\tilde{k}$ on the ratio V_{in}/V_{out} is shown in Fig. 16. For a given θ^*, there is a $\tilde{k}$ limit value at which the volume ratio remains constant. This value corresponds to a stiffness too important for the door (or flap gate) to be pushed by the tide.

For the SRT device, the impact of the float height (given by l_r) on V_{in}/V_{out} is described in Fig. 17. We can see that decreasing the float height (i.e., increasing l_r) leads to a decrease in the volume ratio. Indeed, the lower the float is, the earlier the flap closes in the tide, and the later the flap reopens in the tide. This reduces the water inflow from the estuary.

Discussion

Continuity Solutions

To compare the different devices, we first look at the parameters to be taken into account from a fish passage point of view, in particular the type of opening. To be effective, this opening must satisfy three constraints:

- Size of the opening: The opening must not be smaller than the width of the fish. In addition, the size of the opening plays a role in the number of fish passing; (Kimball et al. 2010) noted more fish passage for an opening of 60 cm than for an opening of 10 cm.
- Position of the opening: Fish species do not swim at the same depth (Bretsch and Allen 2006). It is therefore necessary to ensure that the opening in the structure at the tide is at the depth where the fish swim.
- Time of opening: Fishes do not all swim at the same time of day (Kimball et al. 2017) or tide (Kimball and Able 2012). In order for a fish to pass the structure into the sea, the opening must occur at the time it swims.

These three parameters of the opening (size, position, and time) are easily modified in our models. Reintroductions of salt water loaded with suspended matter, allowed by an opening in a structure at tide, can recreate or improve the habitats of certain estuarine fish species or those living close to the estuary. However, at present, there are too few studies on the subject to quantify the impacts according to the characteristics of an opening (size, position, etc.).

Nevertheless, the following considerations can be extracted from the previous results.
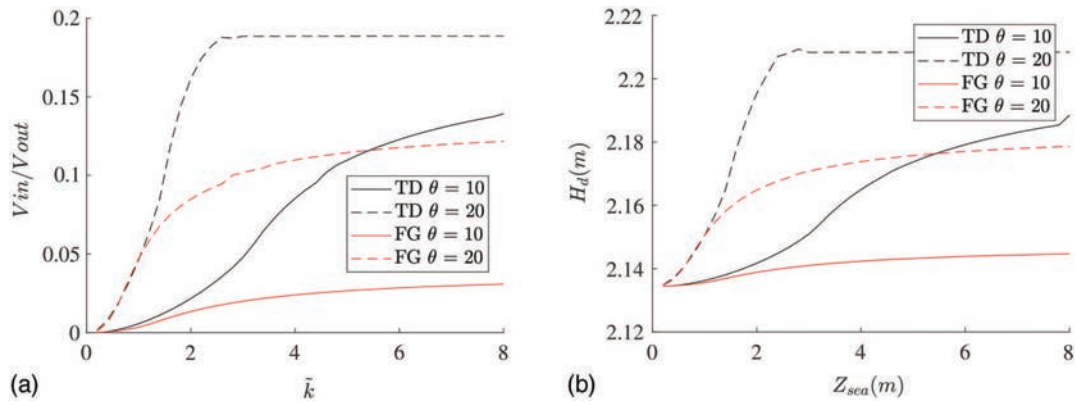
Fig. 16. (Color) Influence of stiffness $\tilde{k}$ on volume ratio and the average of h_d for two different θ angles. The upstream flow is 3 m³/s and the tidal range is 3.5 m.

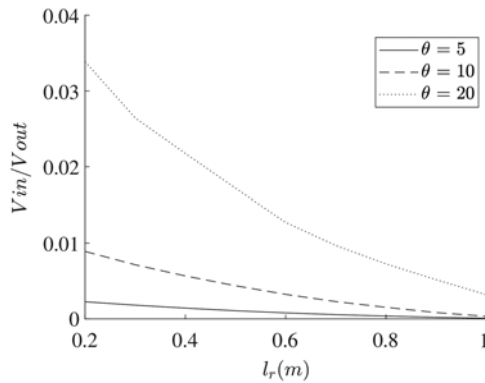**Fig. 17.** Influence of length l_r on volume ratio for three different θ angles. The upstream flow is 3 m³/s and the tidal range is 3.5 m.

Block versus Stiffener

Unlike a block device, a stiffener allows for adaptation to tidal variations. Indeed, with a stiffener it is possible, for example, to define a maximum inflow/outflow volume ratio which is not exceeded for a low and high tidal range. This maximum is adjustable by modifying $\tilde{k}$. A stiffener thus makes it possible to limit the inflow of water coming from the estuary. The disadvantage of a stiffener is the complete closure of the structure to the sea at high tide, whereas certain species could favor this moment of passage. They are therefore more selective in terms of species. The combination of a stiffener and a block has the advantage of adjusting the opening to the inversion, but little data is available to know the best opening for a given species. To respect both the volume ratio and the opening at high tide, a block is sufficient.

Tidal Door versus Flap Gate

With a tidal door, ecological continuity is reestablished throughout the entire depth of the structure. This is important because fish species do not swim at the same depth (Bretsch and Allen 2006). Flap gates give preference to bottom-swimming species. The spatial position of the window for restoring ecological continuity is not neutral.

Float versus Stiffener

For the same volume of incoming water, a float keeps a larger but shorter time opening (at the beginning of the inversion and at the end). Floats leave a more legible entrance (or exit) and taller individuals have more room to pass. They are therefore preferred. Nevertheless, the float seems more sensitive to ice jams and is more difficult to adjust on site. The length of the rods must be planned in advance, whereas the position of the stiffener can be adapted on site.

Use for Other Environmental Issues

The models of tidal hydraulic structures equipped with passage devices presented in this study allow the calculation of the volumes passing through the structure and an estimation of the evolution of the water level in the marshland. This makes it possible to answer a good number of questions that arise when sizing these hydraulic structures for purposes such as the question of flooding or submersion, the tidal range requirements for the flora, and the need to maintain a minimum water level. Similarly, for estuarine water intrusion problems or drainage needs, the models can be used to calculate the volume of water discharged by the structure during a tidal cycle, the volumes of water entering the network from the estuary, and the ratio of these two volumes.

Modeling

Network modeling shows the impact on upstream levels of the combined effect of the tide and the structure. This variation in water level (on the order of 1 m) makes it possible to reproduce asymmetries in hydrographs which are observed in the field that do not appear with a model with a constant reach level. This improves the calculation of passage times during the tide. Asymmetries at high tide also change the flow rate and water level. This leads to different water velocity between the two models. Inaccuracy in velocity has two consequences: a poor understanding of the passage of potential good swimmers and unpredictability of possible silting or erosion in the vicinity of the structure.

A quasi-stationary modeling yielded similar results to the full Saint-Venant solution. It is recommended if the water surface has a constant slope along the canal (for example, in a network with a small channel). In the case of long channels, a complete 1D model (Saint-Venant type) should be used instead. The models of hydraulic structures developed here could be included in standard open-channel software (Baume et al. 2005; Hydrologic Engineering Center 2016) but can also be used as stage discharge relationships for direct discharge estimation.

Conclusion

In this study, a method for dimensioning hydromechanical solutions (stiffeners and floats) to improve the ecological continuity of structures at sea was presented. We numerically studied these solutions, which have not yet been widely used, to highlight their advantages, in terms of management constraints, compared to the conventional solutions which consist of keeping a permanent opening in the structure at high tide. The solution assessment was made by determining the impact on the network level and the volume of water passing through the structure. It was shown that these devices significantly reduce water inflow from the estuary while leaving an opening during part of the high tide. The advance of this work lies mainly in the possibility of quantifying and prioritizing the solutions between them and verifying their operation for different hydrological conditions. Thus, an improvement in the accuracy of the calculations can be obtained by adjusting the discharge coefficients. From this analysis it is possible to quickly have all the forces on the gate and hinges, supports from the kinetic resultant theorem on the x- and y-direction s. This can also be useful for dimensioning (door curvature, for example).

However, in order to allow the dimensioning of these devices with biological constraints, behavioral data must specify the actual conditions that are penalizing for the passage. In this way it will be possible to better discriminate between favorable sizes and opening positions.

Appendix. Modelling Details

Stiffener-Gate Link

Calculations are made in the base with the origin $AR_{A,n,t,z}$. It is not Galilean; however, the movement being plane and A being fixed, the expression of the derivative of the angular momentum on z is the same as in a Galilean base. One introduces the angle of friction ϕ related to the friction coefficient f by $f = \tan\phi$ (Fig. 18).

The force provided by the spring in the direction of its axis x (f_x) is written

$$f_x = F_s \cos(\theta - \phi) \tag{22}$$

where F_s = magnitude for the total spring force on the door.

The projection on $R_{A,n,t,z}$ gives

$$f_n = F_s \cos\phi \tag{23}$$

So

$$f_n = \frac{f_x}{\cos(\theta - \phi)} \cos\phi \tag{24}$$
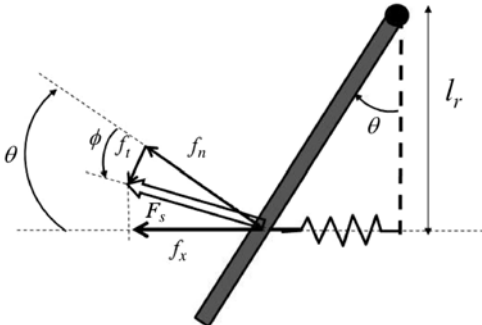

Fig. 18. Decomposition of the force exerted by the spring on the door.

The moment of strength is written

$$\overrightarrow{M_s(A)} = \overrightarrow{AS} \wedge \overrightarrow{F_s} \tag{25}$$

$$\overrightarrow{M_s(A)} = \vec{lt} \wedge (f_n\vec{n} + f_t\vec{t}) \tag{26}$$

$$\overrightarrow{M_s(A)} = f_n \frac{l_r}{\cos\theta}\vec{z} = kl_r^2(\tan\theta - \tan\theta_*)\frac{\cos\phi}{\cos(\theta - \phi)\cos\theta}\vec{z} \tag{27}$$

We will assume $\phi = 0$ (no friction) in the following to simplify the expressions, but if f is known, the same methodology can be applied.

Without friction the moment becomes

$$\overrightarrow{M_s(A)} = kl_r^2(\tan\theta - \tan\theta_*)[1 + \tan^2\theta]\vec{z} \tag{28}$$

In the results presented, it is assumed that there is no friction. This corresponds to a spherical contact part made of smooth metal as installed on the current stiffeners.

Angular Momemtum Theorem

The angular momemtum theorem is applied in A with moments resulting from the integration of the pressure forces on the valve. The lower bound h_{sd} and the upper bound h_{su} depend on the position of the axis of rotation in relation to the tide.

If $h_{su} > h_A$, then $h_{su} = h_A$; otherwise, $h_{su} = h_u$.

By noting l the width of the flap, the moment of the upstream force on the gate can be written

$$\overrightarrow{M_u} = l \int_{h_{sd}}^{h_{su}} \vec{F_u}(M) \wedge \vec{AM} dz \tag{29}$$

On $\vec{z}$, we obtain

$$M_u = l \int_{h_{sd}}^{h_{su}} (p_0 + \rho g(h_u - z))(h_A - z)dz \tag{30}$$

$$M_u = l\left\{ \int_{h_{sd}}^{hs} (p_0 - +\rho g h_u)h_A dz - (p_0 + \rho g h_u)z - (\rho g h_A)z + \rho g z^2 dz \right\} \tag{31}$$

$$M_u = l\left\{ \int_{h_{sd}}^{h_{su}} (p_0 + \rho g h_u)h_A dz - (p_0 + \rho g(h_u + h_A))z + \rho g z^2 dz \right\} \tag{32}$$

$$M_u = l\left\{ (p_0 + \rho g h_u)h_A(h_{su} - h_{sd}) - \frac{1}{2}(p_0 + \rho g(h_u + h_A))(h_{su}^2 - h_{sd}^2) + \frac{1}{3}\rho g(h_{su}^3 - h_{sd}^3) \right\} \tag{33}$$

$$M_u = l(h_{su} - h_{sd})\left\{ (p_0 + \rho g h_u)h_A - \frac{1}{2}(p_0 + \rho g(h_u + h_A))(hs + h_{sd}) + \frac{1}{3}\rho g(h_{su}^2 + h_{sd}^2 + h_{su}h_{sd}) \right\} \tag{34}$$

We define $X_s = h_{su}/hu$, $X_i = h_{sd}/hu$, $X_d = h_d/hu$, and $X_A = h_A/hu$. Then we have

$$M_u = \rho g h_u^3 l(X_s - X_i)\left\{(\tilde{p}_0 + 1)X_A - \frac{1}{2}(\tilde{p}_0 + (1 + X_A)(X_s + X_i)\right.$$
$$\left. + \frac{1}{3}(X_s^2 + X_i^2 + X_s X_i))\right\} \tag{35}$$

For the moment of the downstream force, the integration bounds are $h_{su} = h_A$ if $h_{su} > h_A$ and $h_{su} = h_d$ otherwise.

The equation is the same as for the upstream force but with the opposite sign and with X_d instead of 1 (corresponding to $h = h_u$).

The moment of the air force allows the elimination of the terms in p_0. The balance of the moments is written

$$M_u + M_d + M_w + M_s = -J_A \ddot{\theta} \tag{36}$$

where M_w = moment of the weight, expressed by assuming a rectangular parallelepiped, i.e., a center of gravity at $l/2$; and M_u, M_d, and M_s are the moment due to the force on the upstream plane of the gate, on the downstream plane of the gate, and due to the stiffener, respectively

$$(X_{su} - X_i)\left\{X_A - \frac{1}{2}(1 + X_A)(X_{su} + X_i) + \frac{1}{3}(X_{su}^2 + X_i^2 + X_{su}X_i)\right\}$$
$$- (X_{sd} - X_i)\left\{X_d X_A - \frac{1}{2}(X_d + X_A)(X_{sd} + X_i)\right.$$
$$\left. + \frac{1}{3}(X_{sd}^2 + X_i^2 + X_{sd}X_i)\right\} + \frac{1}{2}\tilde{m}\sin\theta\tilde{l}^3$$
$$+ \tilde{k}\tilde{l}^3(\tan\theta - \tan\theta^*)(1 + \tan^2\theta) = -\frac{J_A\ddot{\theta}}{\rho g h_u^3 l} \tag{37}$$

with $\tilde{m} = m/\rho l^3$, and $\tilde{l}$ and $\tilde{k}$ have the same definition as the case of the tidal door.

Geometric Relationships for SRT Structure Modeling

To show the method for any type of SRT—for example, for the more complicated function $f(h_u)$—we define and determine the value of the angles α and β, which provide the position of the system (Fig. 5)

$$\alpha = \frac{\pi}{2} - \theta \tag{38}$$

$$l_r \cos\alpha = l_c \cos\beta \tag{39}$$

$$\beta = \arccos\left(\frac{l_r}{l_c}\cos\alpha\right) \tag{40}$$

Then the trigonometric relationships linking the different lengths of the problem are written

$$h - h_p = l_f \sin\beta \tag{41}$$

$$h_A - h_p = l_r \sin\alpha \tag{42}$$

Using Eqs. (41) and (42), we can relate the flap opening to the characteristics of the structure and the downstream water level. Finally, we use Eqs. (38) and (40) to express this relation explicitly as a function of θ

$$h_A - h = l_r \sin\alpha - l_f \sin\beta$$
$$= l_r \sin\alpha - l_f \sin\left(\arccos\left(\frac{l_r}{l_c}\cos\alpha\right)\right)$$
$$= l_r \sin\alpha - l_f\sqrt{1 - \left(\frac{l_r}{l_c}\cos\alpha\right)^2}$$
$$= l_r \cos\theta - l_f\sqrt{1 - \left(\frac{l_r}{l_c}\sin\theta\right)^2} \tag{43}$$

Data Availability Statement

Some or all data, models, or code that support the findings of this study are available from the corresponding author upon reasonable request.

References

Amaral, S. D., P. Branco, A. Teixeira da Silva, C. Katopodis, T. Viseu, M. T. Ferreire, A. Nascimento, and J. M. Santos. 2016. "Upstream passage of potadromous cyprinids over small weirs: The influence of key-hydraulic parameters." *J. Ecohydraulics* 1 (1–2): 79–89. https://doi.org/10.1080/24705357.2016.1237265.

Baume, J. P., P. O. Malaterre, G. Belaud, and B. Le Guennec. 2005. "SIC: A 1D hydrodynamic model for river and irrigation canal modeling and regulation," edited by R. C. Vieira da Silva, 1–81. *Métodos Numéricos em Recursos Hidricos*. Coppetec Fundacao, Brasil: Associacao Brasileira de Recursos Hidricos.

Becker, A., M. Holland, J. A. Smith, and I. M. Suthers. 2016. "Fish movement through an estuary mouth is related to tidal flow." *Estuaries Coasts* 39 (4): 1199–1207. https://doi.org/10.1007/s12237-015-0043-3.

Belaud, G., L. Cassan, and J. P. Baume. 2009. "Calculation of contraction coefficient under sluice gate and application to discharge measurement." *J. Hydraul. Eng.* 135 (12): 1086–1091. https://doi.org/10.1061/(ASCE)HY.1943-7900.0000122.

Belaud, G., and X. Litrico. 2008. "Closed-form solution of the potential flow in a contracted flume." *J. Fluid Mech.* 599: 299–307. https://doi.org/10.1017/S0022112008000232.

Bernhard, F. A., and P. Perona. 2017. "Dynamical behavior and stability analysis of hydromechanical gates." *J. Irrig. Drain. Eng.* 143 (9): 04017039. https://doi.org/10.1061/(ASCE)IR.1943-4774.0001209.

Bretsch, K., and D. M. Allen. 2006. "Tidal migrations of nekton in salt marsh intertidal creeks." *Estuaries Coasts* 29 (3): 474–486. https://doi.org/10.1007/BF02784995.

Burrows, R., G. Ockleston, and K. Ali. 1997. "Flow estimation from flap-gate monitoring." *Water Environ. J.* 11 (5): 346–355. https://doi.org/10.1111/j.1747-6593.1997.tb00990.x.

Cassan, L., L. Guiot, and G. Belaud. 2018. "Modeling of tide gate to improve fish passability." In *Proc., of 7th IAHR Int. Symp. on Hydraulic Structures*.
Aachen, Germany: Aachen Univ.

Cassan, L., T. Tien, D. Courret, P. Laurens, and D. Dartus. 2014. "Hydraulic resistance of emergent macroroughness at large Froude numbers: Design of nature-like fishpasses." *J. Hydraul. Eng.* 140 (9): 04014043. https://doi.org/10.1061/(ASCE)HY.1943-7900.0000910.

Chow, V. 1959. *Open-channel hydraulics*. New York: McGraw-Hill.

Doehring, K., R. Young, J. Hay, and A. Quarterman. 2011. "Suitability of dual-frequency identification sonar (DIDSON) to monitor juvenile fish movement at floodgates." *N. Z. J. Mar. Freshwater Res.* 45 (3): 413–422. https://doi.org/10.1080/00288330.2011.571701.

Feunteun, E. 2002. "Management and restoration of European eel population (*Anguilla anguilla*): An impossible bargain." *Ecol. Eng.* 18 (5): 575–591. https://doi.org/10.1016/S0925-8574(02)00021-6.

French, R. H. 1985. *Open-channel hydraulics*. New York: McGraw-Hill.

Giannico, G. R., and J. A. Souder. 2004. *The effects of tide gates on estuarine habitat and migratory fish*. Corvallis, OR: Oregon State Univ.

Giannico, G. R., and J. A. Souder. 2005. Vol. 5 of *Tide gates in the Pacific Northwest: Operation, types, and environmental effects*. Corvallis, OR: Oregon State Univ.

Gibson, R. 2003. "Go with the flow: Tidal migration in marine animals." *Hydrobiologia* 503: 153–161. https://doi.org/10.1023/B:HYDR.0000008488.33614.62.

Henderson, F. 1966. *Open channel flow*. New York: Macmillan.

Hydrologic Engineering Center. 2016. *HEC-RAS, river analysis system, hydraulic reference manual*. Version 5.0. Davis, CA: US Army Corps of Engineers.

Katopodis, C., J. Kells, and M. Acharya. 2001. "Nature-like and conventional fishways: Alternative concepts?" *Can. Water Resour. J.* 26 (2): 211–232. https://doi.org/10.4296/cwrj2602211.

Kimball, M. E., and K. W. Able. 2012. "Tidal migrations of intertidal salt marsh creek nekton examined with underwater video." *Northeastern Nat.* 19 (3): 475–486. https://doi.org/10.1656/045.019.0309.

Kimball, M. E., K. M. Boswell, and L. P. Rozas. 2017. "Estuarine fish behavior around slotted water control structures in a managed salt marsh." *Wetlands Ecol. Manage.* 25 (3): 299–312. https://doi.org/10.1007/s11273-016-9517-8.

Kimball, M. E., L. P. Rozas, K. M. Boswell, and J. H. Cowan, Jr. 2010. "Evaluating the effect of slot size and environmental variables on the passage of estuarine nekton through a water control structure." *J. Exp. Mar. Biol. Ecol.* 395 (1–2): 181–190. https://doi.org/10.1016/j.jembe.2010.09.003.

Larinier, M. 2002. "Pool fishways, pre-barrages and natural bypass channels." *Bull. Fr. Peche Piscic.* 364: 54–82. https://doi.org/10.1051/kmae/2002108.

Laurence, V., W. Bouyssonie, and C. Rigaud. 2015. "Fish-friendly management of first dams in the tidal area of the Gironde estuary." In *Proc., Int. Conf. on Engineering and Ecohydrology for Fish Passage*. Gottingen, Netherlands: International Conference on Engineering and Ecohydrology for Fish Passage.

Lotze, H. K., H. S. Lenihan, B. J. Bourque, R. H. Bradbury, R. G. Cooke, M. C. Kay, S. M. Kidwell, M. X. Kirby, C. H. Peterson, and J. B. Jackson. 2006. "Depletion, degradation, and recovery potential of estuaries and coastal seas." *Science* 312 (5781): 1806–1809. https://doi.org/10.1126/science.1128035.

McCleave, J. D. 1980. "Swimming performance of European eel (*Anguilla anguilla* (L.)) elvers." *J. Fish Biol.* 16 (4): 445–452. https://doi.org/10.1111/j.1095-8649.1980.tb03723.x.

McCleave, J. D., and R. C. Kleckner. 1982. "Selective tidal stream transport in the estuarine migration of glass eels of the American eel (*Anguilla rostrata*)." *ICES J. Mar. Sci.* 40 (3): 262–271. https://doi.org/10.1093/icesjms/40.3.262.

Nilsson, C., C. Reidy, M. Dynesius, and C. Revenga. 2005. "Fragmentation and flow regulation of the world's large river systems." *Science* 308 (5720): 405–408. https://doi.org/10.1126/science.1107887.

O'Shea, T. J., C. A. Beck, R. K. Bonde, H. I. Kochman, and D. K. Odell. 1985. "An analysis of manatee mortality patterns in Florida, 1976–81." *J. Wildl. Manage.* 49 (1): 1–11. https://doi.org/10.2307/3801830.

Ovidio, M., and J. C. Philippart. 2002. "The impact of small physical obstacles on upstream movements of six species of fish." *Hydrobiologia* 483: 55–69. https://doi.org/10.1023/A:1021398605520.

Rampano, B. 2009. *Water control structures: Designs for natural resource management on coastal floodplains*. Sydney, Australia: NSW Dept. of Industry and Investment.

Rigaud, C. 2015. "Continuité biologique et ouvrages soumis á marée: Le cas de l anguille européenne (les éléments importants pour évaluer et agir)." In *Atelier thématique du GRISAM*. Charente-maritime, France: GRISAM.

Rigaud, C., A. Alric, F. X. Robin, and D. Courret. 2014. *Les civelles face á deux ouvrages latéraux de l estuaire de la Charente. tests de modalités de gestion ou d aménagement visant á améliorer la franchissabilité de ces ouvrages. bilan des suivis 2010–2013*. Rapport du Pole Eco-hydraulique de Toulouse (Onema-Irstea-Imft). Toulouse, France: Pole écohydraulique (Onema-Irstea-Imft).

Sinniger, R. O., and W. Hager. 1988. "Traité de Génie Civil de l'Ecole polytechnique fédérale de Lausanne." In Vol. 15 of *Constructions Hydrauliques, ecoulements stationnaires*. Lausanne, Switzerland: Presses polytechniques romandes.

Taylor, A. 2011. *A manual for the design and implementation of passage solutions at weirs, tidal gates and sluices*. Norwich, UK: Environment Agency.

Trancart, T., P. Lambert, E. Rochard, F. Daverat, J. Coustillas, and C. Roqueplo. 2012. "Alternative flood tide transport tactics in catadromous species: *Anguilla anguilla*, *Liza ramada* and *Platichthys flesus*." *Estuarine Coastal Shelf Sci.* 99: 191–198. https://doi.org/10.1016/j.ecss.2011.12.032.

Travade, F., and M. Larinier. 2002. "Fish locks and fish lifts." *Bull. Fr. Peche Piscic.* 364: 102–118. https://doi.org/10.1051/kmae/2002096.